Simulation of Motor Current Waveform as an Index for Aortic Valve Open-Close Condition During Ventricular Support

Khalid A. Alonazi, Nigel H. Lovell, *Fellow, IEEE,* and Socrates Dokos, *Member, IEEE*

***Abstract*—Monitoring of aortic valve (AV) opening and closure during heart pump support by a left ventricular assist device (LVAD) is crucial in preventing adverse events such as thrombus formation near the AV. In this paper, simulations of LVAD motor current waveform were undertaken to evaluate its suitability for ascertaining aortic valve status. A two-dimensional fluid-structure interaction finite-element model is presented to predict AV closure during LVAD outflow, useful in the development of a pump speed controller.**

I. Introduction

More than 5 million people will develop some degree of heart failure (HF) in their life time in the United States, where its prevalence averages 2.1% of the normal population [1]. Currently, left ventricular assist devices (LVADs) represent promising therapies for congestive HF patients [2]. Due to the shortage of appropriate heart donors, LVADs are often used as a bridge to transplant, or more frequently nowadays, a destination therapy [3]. Increased use of LVADs for long-term mechanical support necessitates a better understanding of hemodynamic changes in the left ventricle (LV), as well as the timing of aortic valve (AV) closure and opening [4].

Development of valve abnormalities after LVAD placement is common among patients with advanced heart failure, likely due to the fact that the LVAD induces significant changes in hemodynamics by altering the direction of blood flow from the apex of the heart, largely bypassing the LV, directly to the aorta. This abnormal recirculation modifies pressure and stress on the AV, leading to remodeling of the valve [5]. AV functional problems, including aortic insufficiency (AI), prolonged valve closure, and aortic stenosis (AS), are more common in the LVAD patient after implantation [6, 7]. Furthermore, 50% of patients with pulsatile LVADs develop AI or AS within 6–12 months of LVAD implantation [8]. Similarly, a major consequence of the LVAD is excessive flow, resulting in diminished and infrequent AV opening, which could also extend to the systolic phase reducing cardiac output and increasing LV preload [9]. Therefore, it is important to detect any abnormalities in LV hemodynamics due to over-pumping, reduction in preload, or pump regurgitation. Computational modeling of blood flow has been used extensively to study AV hemodynamics. Several finite-element (FE) models of the left ventricle and aortic valve have been developed to simulate leaflet motion during blood flow [10-13]. However, these models did not include heart–pump interaction or simulate AV closure during LVAD support. Although other studies have attempted to model the interaction between the circulatory system and a heart assist pump [14, 15], none of these simulate AV closure during LVAD support.

In the present study, we attempted to evaluate AV state using the LVAD motor current waveform as an index, simulated from a 2D simplified computational model of AV dynamics (closure/opening) under heart pump support. Such a model will be useful in the design and evaluation of physiological pump control algorithms to achieve the balance between LVAD pumping and mechanical circulatory support against disruption to AV movement, which may lead to various AV pathologies. Therefore, the objective of this paper was to investigate how the motor electrical current profile changes with AV state and pump speed. Identifying the AV state according to motor current signal could provide an input to a pump speed controller to prevent highly negative pressure in the left ventricle leading to wall suction, as well as ensuring the AV opens and closes over the cardiac cycle.

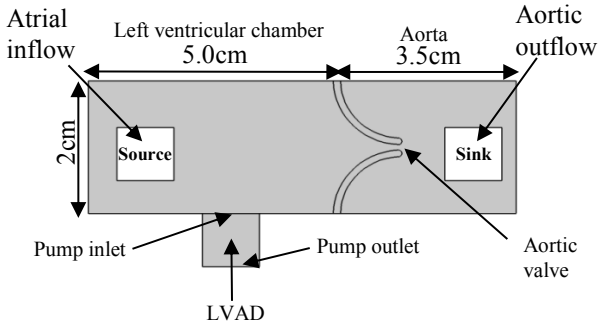

Figure 1. Two-dimensional simplified representation of the left ventricle, aortic valve and pump cannula.

II. Methods

A. Model Description

A two-dimensional fluid structure interaction (FSI) model of aortic valve dynamics was implemented using COMSOL Multiphysics (COMSOL AB, Sweden, Version 4.3a), using the Arbitrary Lagrangian–Eulerian (ALE) method first proposed by Donea *et al.* [16]. ALE is most commonly used for simulating the interaction between moving objects and fluid flow. The model geometry consists of a horizontal flow channel of diameter 2.0 cm representing the ventricle, and narrow curved structures representing the AV leaflets, as shown in Fig. 1. Key model parameters were: blood density 1.06×10^{3} kg/m^{3}, blood viscosity 1.00×10^{-3} Pa.s, leaflet

Khalid A. Alonazi, Socrates Dokos and Nigel H. Lovell are with the Graduate School of Biomedical Engineering, University of New South Wales, Sydney, NSW 2052 Australia (phone: +61-2-9385-9406; email: s.dokos@unsw.edu.au).

density 1.06×10^3 kg/m^3, aortic leaflet Young's modulus 4.7×10^7 Pa and leaflet Poisson's ratio 0.49. The AV consists of two flexible leaflets of length 1.25 cm and thickness 0.1 cm. A thin-walled cannula of width 0.8 cm and length 0.8 cm is inserted into the ventricular chamber wall: these values were adapted from [17]. The model also includes blood inflow into the LV on boundaries placed at the left end of the channel (labelled as "source" in Fig. 1); aortic outflow was modeled as a varying pressure boundary condition (labelled "sink" in Fig. 1). Inward flow at the atrial "source" boundaries was simulated using a Windkessel model of the circulation, connecting the aortic "sink" and the atrial "source" boundaries. These equations governing the Windkessel circuit were implemented as global differential equations in the COMSOL solver. In this study, heart wall contraction on the upper boundary of the ventricular chamber was also incorporated.

B. Model Equations

1) Ventricle model

We characterise blood pulsatile flow as being laminar, Newtonian, viscous and incompressible. The fluid is described by the Navier-Stokes equations for incompressible flow:

$$\rho\left(\frac{\partial \mathbf{u}}{\partial t}+\mathbf{u}\,.\nabla\mathbf{u}\right)=-\nabla p+\mu\nabla^2\mathbf{u}$$
$$\nabla.\,\mathbf{u}=0 \quad (1)$$

where ρ is the fluid density, μ is the viscosity, **u** is the velocity of the fluid and *p* is the pressure.

The fluid flows into the ventricle from the left source (inlet) boundaries. At this entrance, the flow is assumed to have fully developed a laminar profile, changing with time as described in the next section. The valves were modeled as a linear elastic material, formulated as an isotropic Hookean elastic solid expressed using Einsteinian indicial notation as:

$$\varepsilon_{ij}=\frac{1+v}{E}\sigma_{ij}-\frac{v}{E}\sigma_{\alpha\alpha}\delta_{ij} \quad (2)$$

where E is the Young's modulus, v is Poisson's ratio, ε, σ are the Cauchy strain and stress tensors respectively, and δ_{ij} represents of the Kronecker-delta tensor such that:

$$\delta_{ij}=\begin{cases}0 & i\neq j\\ 1 & i=j\end{cases}$$

2) Windkessel model

To simulate the systemic circulation, a simple Windkessel model was employed, characterized by the following equations:

$$P=P_{out}+P_S \quad (3)$$
$$Q_{out}+Q_P=\frac{P_S}{R_S}+C_S\frac{dP_S}{dt} \quad (4)$$
$$P_{out}=Q_{out}\,R_{out}+P_S+(Q_{out}+Q_P) \quad (5)$$

where P is the aortic pressure, P_{out} is the left ventricular outlet pressure, P_S is the systemic pressure, Q_P is the pump flow rate (L/min), Q_{out} is the blood flow ejected from the LV, R_{out} is the characteristic aortic impedance, R_S is the peripheral resistance and C_S is the systemic compliance. The following values were employed for these parameters: R_{out}= 0.014mmHg.s/cm^3, R_S=0.69 mmHg.s/cm^3 and C_S=2.63cm^3/ mmHg: these parameters values were adapted from [18], which were adjusted from those reported [19], based on our simulations with our modified model.

3) Pump model

The differential pressure head (ΔP) across the pump outlet is modeled using three equations as reported by Lim *et al.* [15]; the motor windings electrical equation (6), the electromagnetic torque transfer equation (10), and the pump hydraulic equation linear equation (11).

a) Motor windings electrical equation

$$V=I(R+jX)+E \quad (6)$$

where V is the motor terminal voltage, I is the motor current, R is motor winding resistance and X is the motor winding reactance. E is the back electromotive force (BEMF) given by:

$$E=k_e\omega_e \quad (7)$$

where k_e= 8.48mV/rad and ω_e is the electrical speed ($\omega_e=2\omega$, where ω is the impeller speed in rad/s).

Due to the synchronization between BEMF and motor electrical current to produce maximum torque efficiency, equation (6) can be written as:

$$L\frac{dI}{dt}=-k_e\omega_e-RI-V \quad (8)$$

where R = 1.38 Ω is the motor winding resistance and L = 0.439 mH is the motor winding inductance. V was determined using a proportional controller to track the desired pump speed according to:

$$V=K(\omega_{set}-\omega_e) \quad (9)$$

where K is constant and ω_{set} is the pump speed set point.

b) Electromagnetic torque transfer equation

$$T_e=J\frac{d\omega}{dt}=3k_e\omega_e-(c_1{Q_P}^2\omega+c_2Q_P\omega^2+c_3+c_4\omega^3) \quad (10)$$

where T_e is the output electromagnetic torque, Q_P is the pump flow rate (L/min), and J is the moment of inertia of the impeller. The coefficients c_1, c_2, c_3 and c_4 are viscosity-dependent parameters.

C) Pump hydraulic equation

$$\Delta P=c_0+c_5{Q_P}^3+c_6\omega^2 \quad (11)$$

where c_5, c_6, c_0 are viscosity-dependent parameters. In this paper, we assume that the viscosity remains constant throughout the simulation.

C. Boundary Conditions

Fluid flow boundary conditions of the model included the following: a sinusoidal flow pattern with period 1 Hz and amplitude 50 mL/s was applied at the inlet (source) boundaries, 0 mmHg pressure was specified at the outlet (sink) boundaries, a pressure of $P_S-\Delta P$ was applied at the outflow of the pump cannula, the fixed walls of the model were set to be no-slip boundaries, and the valve leaflets were assigned a 'moving-wall' boundary condition, whereby the velocity the fluid at these leaflet boundaries was set equal to the velocity of the moving wall. The stress on the valve

leaflet boundaries was set to equal the fluid stress, with the leaflet root boundaries fixed. Finally, heart wall contraction was simulated by moving the upper boundary of the ventricular chamber according to:

$$v = v_{max} sin\left(\pi \frac{x}{L}\right) sin(\pi f t) \quad (12)$$

where v is the wall velocity, x is the x coordinate, v_{max} is the maximum velocity, and L is the total length of the upper boundary segment. As with the valve leaflets, the fluid velocity at this boundary was set equal to the wall velocity.

D. Computational Settings

The FSI simulations were performed on a 3.20 GHz Intel Core i7-3930K PC workstation, using a 64-bit Windows platform, with an applicable memory allocation of 32 GB. The fully-meshed model exhibited approximately 65,500 degrees of freedom.

III. Results and Discussion

The model behavior could effectively be divided into two phases: aortic valve closed and open, as shown from pump motor current in Fig. 2 (a,b). The valve ejection phase (VE) was characterized by two waveforms: the pump motor current and the pump speed. In each simulation, the impeller speed set point was increased from 50 rad/s to 200 rad/s in 50 rad/s increments in order to cover the full range of pumping state transitions (from ventricular ejection (VE) to aortic valve closed (VC)). The physiological signals, instantaneous pump impeller speed (ω) and motor current (I), were monitored and recorded from the pump model. Fig. 2 shows the waveform obtained from two different set points of 100 rad/s and 150 rad/s. It shows the relation between the peak motor current and instantaneous pump speed in our 2D model, revealing an inverse correlation with the pump speed. In addition, the relationship between motor current amplitude and LV pressure exhibited an excellent correlation: as shown in Fig. 4, peak motor current increased with increases in LV systolic pressure as confirmed by previous mock-loop [20] and *in-vivo* [21] studies. Transition from state VE to state VC occurred with increasing pump speed, where the VE state corresponds to left ventricular ejection during systole. However, during increase of the pump speed set point to 200 rad/s, VC state was continuously maintained, in which the

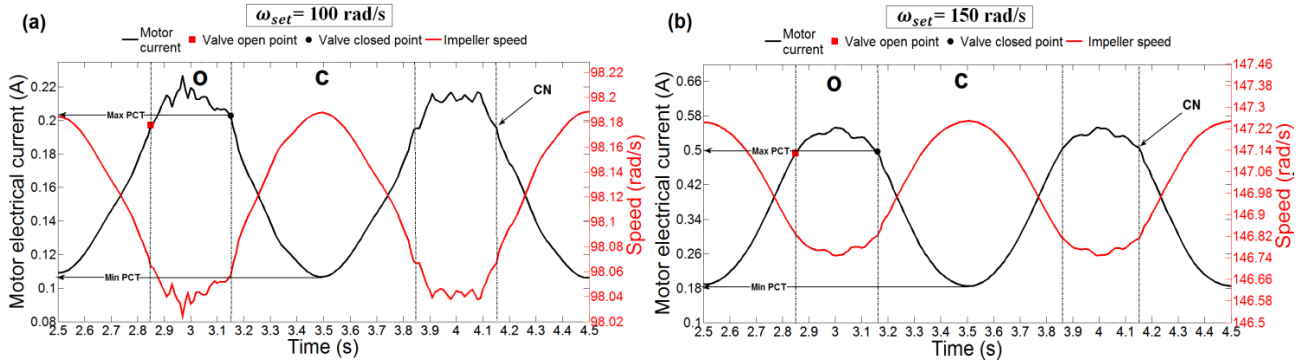

Figure 2. Simulated electric current and pump impeller speed at two motor speed set points (100 and 150 rad/s), where ' ■ ' and ' ● ' indicate AV opening and closing times, respectively, (a). the periods 'O' and 'C' represent the period during which the AV is open, referred to as ventricular ejection (VE), and valve closed (VC), respectively (ω_{set} = 100 rad/s), (b). the periods 'O' and 'C' represent the periods during which the AV is open and closed, respectively (ω_{set} = 150 rad/s). Max PCT and Min PCT are maximum and minimum points of current threshold during AV closure, respectively. The motor current waveform at Max PCT begins to decrease more rapidly once the aortic valve is closed at the closing notch (CN).

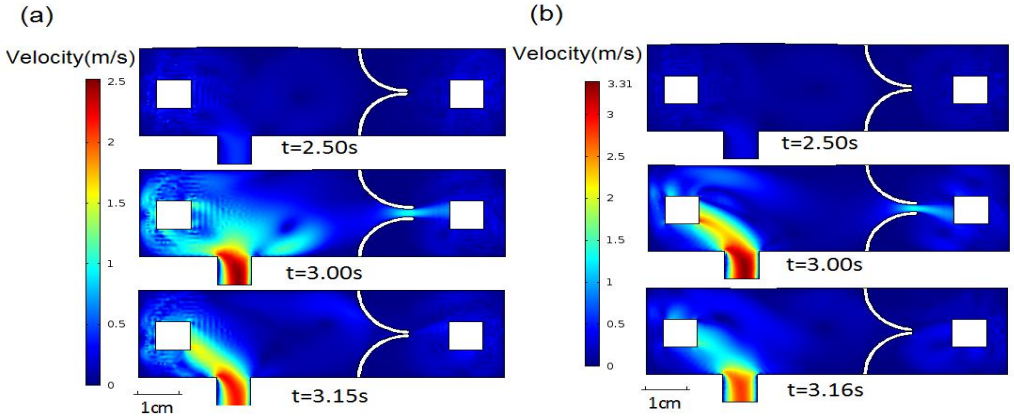

Figure 3. Snapshots of simulated LV blood velocity magnitude during LVAD support at various phases during the cardiac cycle. (a) Aortic valve closing and opening phases for ω_{set}= 100 rad/s. (b) Aortic valve movement for ω_{set}= 150 rad/s.

AV remained closed with no blood flow to the proximal aorta. Furthermore, a high motor current of 0.203 A was observed during the AV closing phase (t=3.15s) with ω_{set} = 100 rad/s, decreasing rapidly throughout the AV closed state (t=3.15-3.85s), reaching a minimum value of 0.1067A at t=3.49s. Fig. 3 shows simulation results of AV movement

during LVAD support, where the opening time is approximately the same at both speed set points. However, the closure time was delayed by 10 ms at a motor speed set point of 150 rad/s. In addition during AV opening, there were small oscillations in the current waveform, probably due to mechanical flutter of the valve leaflets.

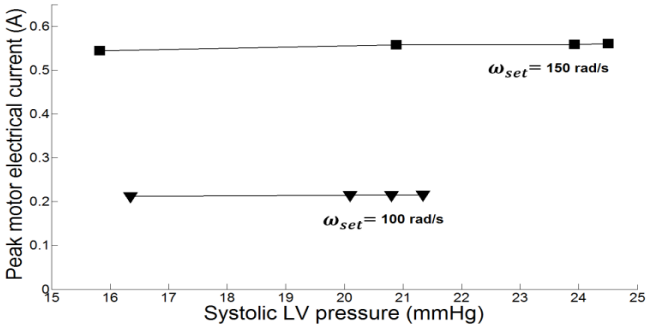

Figure 4. LV systolic pressure – peak LVAD motor current relationship in simplified model.

In terms of simulations of the mechanics of the left ventricle, the real heart exhibits more complex motion and can be modelled with more realistic active contractile properties, such as a time-varying elastance. This may affect the times AV open-close. However, such more detailed modelling was beyond the scope of this study. Furthermore, the model may be extended in future to incorporate a range of heart failure conditions including changes in cardiac contractility, systemic vascular resistance and total blood volume.

IV. Conclusions

We have presented a simplified two-dimensional FSI model of the aortic valve and ventricle during LVAD support, based on the ALE method. The model was formulated with the aim of providing insights into the dynamics of heart-pump interaction, and to simulate LVAD motor current waveform in relation to AV state. The results confirmed that when the AV opens, there is a higher motor current compared to when the valve is closed. This motor current result is similar to that obtained by Lim *et al*. [15]. However, our computational model of motor current variations during AV movement, particularly during its closing phase, and under pulsatile flow conditions, will provide significant insights into LV function during LVAD support, particularly as the model is further developed to incorporate realistic anatomies. Moreover, our simulations offer the potential of improving current LVAD control systems to ensure patient safety and comfort, and reduce the incidence of AV pathologies during heart pump support.

References

[1] A. S. Go, D. Mozaffarian, V. L. Roger, E. J. Benjamin, J. D. Berry, M. J. Blaha*, et al.*, "Heart disease andstroke statistics--2014 update: A report from the American Heart Association," *Circulation,* vol. 18, p. 18, 2013.

[2] G. Sayer, Y. Naka, and U. P. Jorde, "Ventricular assist device therapy," *Cardiovascular Therapeutics,* vol. 27, pp. 140-150, 2009.

[3] F. Arabia, R. Smith, D. Rose, D. Arzouman, G. Sethi, and J. Copeland, "Success rates of long-term circulatory assist devices used currently for bridge to heart transplantation," *ASAIO Journal (American Society for Artificial Internal Organs: 1992),* vol. 42, p. M542, 1996.

[4] M. McCormick, D. Nordsletten, D. Kay, and N. Smith, "Modelling left ventricular function under assist device support," *International Journal for Numerical Methods in Biomedical Engineering,* vol. 27, pp. 1073-1095, 2011.

[5] J. T. Butcher, C. A. Simmons, and J. N. Warnock, "Review—Mechanobiology of the aortic heart valve," *J Heart Valve Dis,* vol. 17, 2008.

[6] A. G. Rose, S. J. Park, A. J. Bank, and L. W. Miller, "Partial aortic valve fusion induced by left ventricular assist device," *The Annals of Thoracic Surgery,* vol. 70, p. 1270, 2000.

[7] G. V. Letsou, J. H. Connelly, R. M. Delgado III, T. J. Myers, I. D. Gregoric, F. W. Smart*, et al.*, "Is native aortic valve commissural fusion in patients with long-term left ventricular assist devices associated with clinically important aortic insufficiency?," *The Journal of Heart and Lung Transplantation,* vol. 25, pp. 395-399, 2006.

[8] S. J. Park, K. K. Liao, R. Segurola, K. Madhu, and L. W. Miller, "Management of aortic insufficiency in patients with left ventricular assist devices: a simple coaptation stitch method (Park's stitch)," *The Journal of Thoracic and Cardiovascular Surgery,* vol. 127, p. 264, 2004.

[9] M. S. Slaughter, J. G. Rogers, C. A. Milano, S. D. Russell, J. V. Conte, D. Feldman*, et al.*, "Advanced heart failure treated with continuous-flow left ventricular assist device," *New England Journal of Medicine,* vol. 361, pp. 2241-2251, 2009.

[10] C. S. Peskin, "The fluid dynamics of heart valves: experimental, theoretical, and computational methods," *Annual Review of Fluid Mechanics,* vol. 14, pp. 235-259, 1982.

[11] H. Watanabe, T. Hisada, S. Sugiura, J.-I. Okada, and H. Fukunari, "Computer simulation of blood flow, left ventricular wall motion and their interrelationship by fluid-structure interaction finite element method," *JSME International Journal. Series C, Mechanical Systems, Machine Elements and Manufacturing,* vol. 45, pp. 1003-1012, 2002.

[12] J. De Hart, G. W. Peters, P. J. Schreurs, and F. P. Baaijens, "A two-dimensional fluid–structure interaction model of the aortic value," *Journal of Biomechanics,* vol. 33, pp. 1079-1088, 2000.

[13] J. De Hart, G. Peters, P. Schreurs, and F. Baaijens, "A three-dimensional computational analysis of fluid–structure interaction in the aortic valve," *Journal of Biomechanics,* vol. 36, pp. 103-112, 2003.

[14] L. Xu and M. Fu, "Computer modeling of interactions of an electric motor, circulatory system, and rotary blood pump," *ASAIO Journal,* vol. 46, pp. 604-611, 2000.

[15] E. Lim, S. L. Cloherty, J. A. Reizes, D. G. Mason, R. F. Salamonsen, D. M. Karantonis*, et al.*, "A dynamic lumped parameter model of the left ventricular assisted circulation," in *Engineering in Medicine and Biology Society, 2007. EMBS 2007. 29th Annual International Conference of the IEEE*, 2007, pp. 3990-3993.

[16] J. Donea, S. Giuliani, and J. Halleux, "An arbitrary Lagrangian-Eulerian finite element method for transient dynamic fluid-structure interactions," *Computer Methods in Applied Mechanics and Engineering,* vol. 33, pp. 689-723, 1982.

[17] D. M. McQUEEN, C. S. Peskin, and E. L. Yellin, "Fluid dynamics of the mitral valve: physiological aspects of a mathematical model," *American Journal of Physiology-Heart and Circulatory Physiology,* vol. 242, pp. H1095-H1110, 1982.

[18] J. M. Jacobsen, P. T. Adeler, W. Y. Kim, K. Houlind, E. M. Pedersen, and J. K. Larsen, "Evaluation of a 2D model of the left side of the human heart against magnetic resonance velocity mapping," *Cardiovascular Engineering: An International Journal,* vol. 1, pp. 59-76, 2001.

[19] A. Cappello, G. Gnudi, and C. Lamberti, "Identification of the three-element windkessel model incorporating a pressure-dependent compliance," *Annals of Biomedical Engineering,* vol. 23, pp. 164-177, 1995.

[20] D. Kikugawa, "Evaluation of cardiac function during left ventricular assist by a centrifugal blood pump," *Artificial Organs,* vol. 24, pp. 632-635, 2000.

[21] D. Kikugawa, "Motor current waveforms as an index for evaluation of native cardiac function during left ventricular support with a centrifugal blood pump," *Artificial Organs,* vol. 25, pp. 703-708, 2001.